

# AN IMPROVED eRHIC INTERACTION REGION DESIGN WITHOUT HIGH FIELD Nb<sub>3</sub>Sn MAGNETS \*

B. Parker<sup>†</sup>, R. B. Palmer and H. Witte, Brookhaven National Laboratory, Upton, New York, USA

## Abstract

The Electron-Ion Collider (EIC) is envisioned as the next DOE Nuclear Physics facility. BNL is proposing eRHIC, a facility based on the existing RHIC complex as a cost effective realization of the EIC project with a peak luminosity of  $10^{34} \text{ cm}^{-2}\text{sec}^{-1}$ . An electron storage ring with an energy range from 5 to 18 GeV will be added in the existing RHIC tunnel. The beams will collide in up to two Interaction Regions (IRs). Balancing conflicting experimental physics and machine accelerator physics demands with realistic eRHIC IR magnet designs requires new concepts and careful attention to detail. We review recent work aimed at reducing IR magnet cost and at avoiding risk associated with using a high-field Nb<sub>3</sub>Sn actively shielded quadrupole that was present in an earlier design.

## ERHIC IR DESIGN REQUIREMENTS

The EIC requirements for eRHIC, as derived from a U.S. Nuclear Physics community White Paper, are:

- An electron-proton center-of-mass energy range of 30 to 140 GeV achieved with proton energies of 41 to 275 GeV and electron energies of 5 to 18 GeV;
- Electron-proton luminosity of  $10^{32}$  to  $10^{34} \text{ cm}^{-2}\text{sec}^{-1}$ ;
- Spin polarized electron and light ion (p, deuteron, <sup>3</sup>He) beams;
- Proton and electron polarization levels of at least 70 percent and arbitrary spin patterns in both beams;
- A wide range of ion species from protons to uranium.

These overarching eRHIC design parameters are described in more detail elsewhere [1-3].

The eRHIC IR design, shown schematically in Figure 1, has multiple requirements and design considerations:

- Focus both electron and hadron beams to small spot sizes at the interaction point (IP), with  $\beta$ -functions down to a few centimeters;
- Initiate beam separation in a Crab Crossing geometry configuration with 25 mrad total crossing angle;
- Separate  $10\sigma$  circulating hadron beam from both a  $\pm 4$  mrad forward neutron cone passed to a Zero Degree Calorimeter (ZDC) and  $\pm 1.3$  GeV/c transverse momentum protons measured at Roman Pot stations;
- Luminosity measurement uses Bethe-Heitler photons from IP split off from the circulating electron beam;
- Scattered electrons, outside the  $15\sigma$  electron beam envelope, are detected at a dedicated electron tagger.
- We must preserve a  $\pm 4.5$  m stay clear region about the IP solely for experimental detector components;
- Synchrotron radiation (synrad) must pass cleanly through the detector and rear side electron magnets to

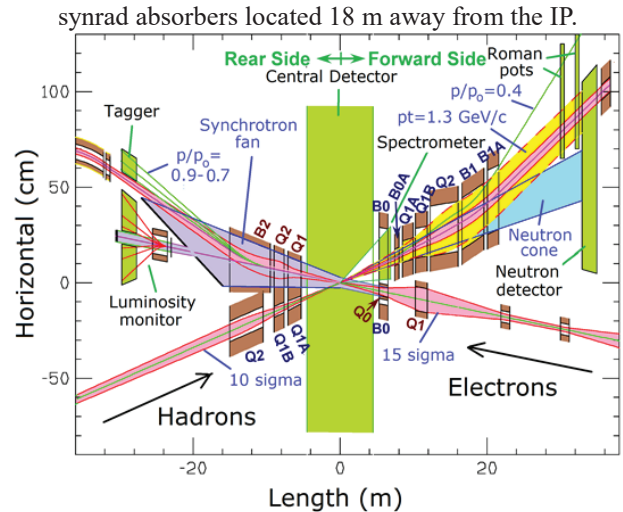


Figure 1: Top view of the central 60 m eRHIC IR region. Note very different scales on the two axes. We use the HERA convention: elements on outgoing proton/ion side of detector are “forward,” while those on incoming side are “rear.” Crossing angle is 25 mrad with beam envelopes shown at:  $10\sigma$  for 275 GeV protons and  $15\sigma$  for 18 GeV electrons.

Since a wide range of forward charged and neutral particles must reach the Roman Pots and ZDC, the forward side hadron magnets apertures are much larger than those needed just for the  $10\sigma$  circulating beam on the rear side. Table 1 details the forward side magnet parameters. Note that with two exceptions the forward side electron and hadron magnets are staggered and do not overlap.

Table 1: Forward side magnet parameters for 275 GeV protons and 18 GeV electrons. Names with B are dipoles, Q are quadrupoles.  $S_{mid}$  is the distance from the IP to the middle of the magnet. Magnets sharing a common yoke are grouped together.  $B_{pole}$  is  $|B|$  for dipoles and the product of gradient times aperture radius for quadrupoles.

Name	$S_{mid}$ (m)	$L_{mag}$ (m)	$R_{ap}$ (mm)	$B_{pole}$ (T)
B0PF	5.9	1.20	200	1.3
Q0EF			25	0.3
B0APF	7.7	0.60	46	3.3
Q1APF	9.2	1.46	56	4.1
Q1BPF	11.1	1.61	78	5.2
Q1EF			63	0.5
Q2PF	14.2	3.80	131	5.3
B1PF	18.1	3.00	135	3.4
B1APF	20.8	1.50	168	2.7

\* Work supported by Brookhaven Science Associates, LLC under Contract No. DE-SC0012704 with the U.S. Department of Energy.

<sup>†</sup> parker@bnl.gov

Content from this work may be used under the terms of the CC BY 3.0 licence (© 2019). Any distribution of this work must maintain attribution to the author(s), title of the work, publisher, and DOI

The first magnet, the B0PF spectrometer dipole, is special in that, as shown in Figure 2, it contains the forward electron quadrupole, Q0EF, inside its main aperture. B0PF also has detectors intended to measure forward particles in an angular range that goes below the lower limit of the main solenoid (about 25 mrad) but above the range that can pass through the next six superconducting IR magnets (about 5 mrad). The Q0EF magnet is shielded from the B0PF dipole field via a bucking dipole [4]. We plan to keep the B0PF field constant at 1.3 T and to use a combination of B0APF and B1PF to close a local orbit bump for hadron energies over the 41 to 275 GeV range.

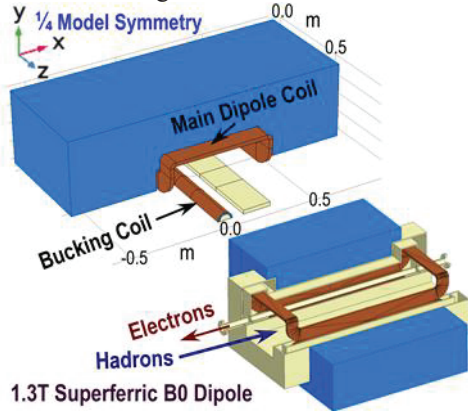


Figure 2: B0PF spectrometer magnet with electron Q0EF magnet inside its main aperture. B0PF is needed for momentum analysis of particles from physics events and covers a critical intermediate angular acceptance range.

For all the hadron IR magnets, a fundamental consideration is that the electron beam must be protected from potentially very strong hadron magnet external fields in order not to perturb the electron beam optics or generate excessive synrad. The combination of strong hadron focusing gradients and the large apertures for experimental acceptance can easily lead to coil fields greater than can be accommodated by conventional NbTi superconductor at 4.5K. This was the case for an initial IR design that used a high gradient Nb<sub>3</sub>Sn main coil surrounded by a larger NbTi active shield coil [5,6]. The active shield kept a large external B-field, associated with an over 8 T coil field, from reaching the electron beam; however, after evaluating the cost and risk of the R&D program to make a Nb<sub>3</sub>Sn coil with new cable and a compact inner support structure we started exploring alternative optics solutions.

The original strong Q1PF quadrupole is split, in the present layout, into two longer but lower-gradient quadrupoles, Q1APF and Q1BPF, with these magnets starting further from the IP. The combination of lower gradient and greater aperture separation means that these quadrupoles can use standard NbTi conductor and now there is sufficient yoke material between the apertures to shield the external field without need for any active shields; however, since Q1APF/Q1BPF take up greater longitudinal space than the original high gradient Q1PF, the Q1EF electron magnet coil must overlap at least one hadron magnet; so the Q1BPF and Q1EF magnets coils share a common yoke structure as shown in Figure 3.

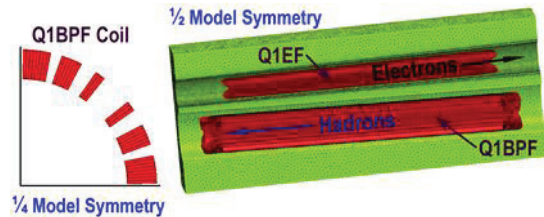


Figure 3: Q1BPF/Q1EF dual aperture magnet with side-by-side quadrupole coils that share a common yoke.

The greatest challenge in providing the hadron magnets is the need to provide the large hadron apertures shown on Figure 1 and listed in Table 1 that are much larger than the 10 $\sigma$  beam size. Since for a given magnet the aperture limitation typically occurs mostly at the downstream end, we can offset and rotate the hadron magnets with respect to the circulating beam to minimize all the hadron magnet apertures (for the quadrupoles this reduces the coil peak field). This trick gains most of the benefit of using tapered magnet apertures/coils without the added complexity of having to taper a collared magnet coil structure. The final separation of the forward neutral and charged particles shown in Figure 1 is achieved due to the combined beam deflection given by the B1PF and B1APF dipoles. As a practical matter B1APF was split off from B1PF to keep a design figure of merit, mid-plane azimuthal force per unit length (i.e.  $B\text{-field}^2 \times \text{Aperture}$ ) consistent with previous RHIC D0 and DX dipole design experience.

Table 2: Rear side magnet parameters for 275 GeV protons and 18 GeV electrons. Names with B are dipoles, Q are quadrupoles.  $S_{mid}$  is the distance from the IP to the middle of the magnet. Magnets sharing a common yoke are grouped together. For tapered magnet apertures the initial radius,  $R_{1ap}$ , is smaller than the final radius,  $R_{2ap}$ .  $B_{pole}$  is  $|B|$  for dipoles and the product of gradient times the final aperture radius for quadrupoles.

Name	$S_{mid}$ (m)	$L_{mag}$ (m)	$R_{1ap}$ (mm)	$R_{2ap}$ (mm)	$B_{pole}$ (T)
Q1APR	6.2	1.80	21	21	1.8
Q1ER			66	80	1.2
Q1BPR	8.3	1.40	28	28	2.3
Q2ER			83	94	1.3
Q2PR	12.2	5.50	50	50	1.4
B2ER			98	139	0.2

The parameters for the rear side magnets are listed in Table 2. With a few caveats the rear side magnets designs are much less demanding than those of the forward side. The first few hadron and electron magnets on the rear side are all side by side and have large electron apertures in order to pass the full synrad fan generated in the upstream electron IR quadrupoles. By passing this synrad fan on to absorbers far from the detector we look to avoid synrad backscatter background issues experienced for the HERA-II upgrade commissioning. Figure 4 shows a typical rear side magnet cross section, that of Q1ER/Q1APR. Now since this rear side hadron magnet only needs to

accommodate the  $10\sigma$  circulating hadron beam, the hadron aperture is smaller than that for the electron beam. The rear side hadron quadrupole coil peak fields are much smaller than their forward side counterparts and it would seem that compared to the forward side we could get by with a smaller yoke thickness between the two apertures. Fortunately, the rear side magnetic fields are all small enough that we can with confidence profitably use the established BNL Direct Wind technique to wind these magnets [7]. Direct Wind allows us to fabricate coils in a wide variety of lengths and apertures without the need to invest in new tooling for each magnet type.

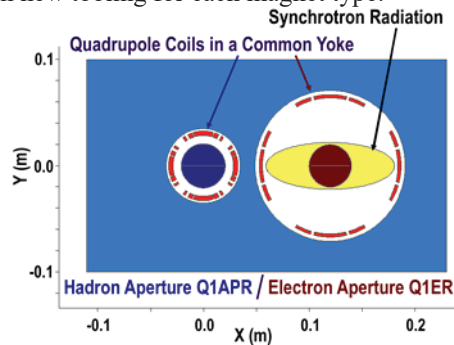


Figure 4: A dual aperture rear side magnet example.

Unfortunately, the electron aperture requirement to fit the synrad fan grows so rapidly with distance from the IP, that in order to maintain even a minimal yoke between the apertures, we are forced to taper all of the rear side electron magnet apertures and their corresponding superconducting coils. But unless special measures are taken, the field strength changes (drops) as the coil radius increases. By playing games and dramatically stretching out one coil end, this drop in local transfer function can be partially offset; however, we adopt a much more flexible approach as illustrated by the tapered coil shown in Figure 5.

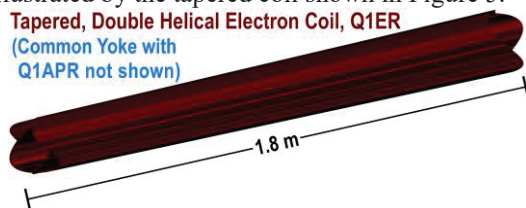


Figure 5: Rear side tapered electron magnet coil that uses a double helical quadrupole winding pattern, with variable conductor pitch, to compensate the local change in gradient due to changes in coil radius along the magnet.

The electron coil tapered winding shown in Figure 5 uses a double helical pattern with two nested solenoid-like coil layers that go around their common axis in opposite directions so that there is no net solenoidal field [8]. By appropriately modulating the winding of the conductor in each coil layer we can create a net transverse dipole or quadrupole field. Local field strength is directly related to local conductor pitch differences in the two layers and by smoothly changing the pitch we can keep the field strength constant along the magnet's length despite changes in coil radius. R&D is now in progress to wind such a tapered coil via BNL Direct Wind technology.

## REFERENCES

- [1] V. Ptitsyn, M. Blaskiewicz, A. Fedotov, C. Montag, F. Willeke, "eRHIC Luminosity for Various Operational Scenarios", presented at the 10th International Particle Accelerator Conf. (IPAC'19), Melbourne, Australia, May 2019, paper MOPRB102, this conference.
- [2] W. Fischer *et al.*, "eRHIC in Electron-Ion Operation," presented at the 10th International Particle Accelerator Conf. (IPAC'19), Melbourne, Australia, May 2019, paper MOPRB072, this conference.
- [3] C. Montag *et al.*, "eRHIC Electron Ring Design Status," presented at the 10th International Particle Accelerator Conf. (IPAC'19), Melbourne, Australia, May 2019, paper MOPRB093, this conference.
- [4] H. Witte, R.B. Palmer and B. Parker, "Options for the Spectrometer Magnet of the eRHIC IR", in *Proc. IPAC'18*, Vancouver, BC, Canada, Apr.-May 2018, pp. 2401-2403.
- [5] B. Parker, R.B. Palmer, and H. Witte, "The eRHIC Interaction Region Magnets", in *Proc. 8th Int. Particle Accelerator Conf. (IPAC'17)*, Copenhagen, Denmark, May 2017, paper WEPVA151, pp. 3624-3626.
- [6] B. Parker *et al.*, "Fast Track Actively Shielded Nb<sub>3</sub>Sn IR Quadrupole R&D," in *Proc. the 9th International Particle Accelerator Conf. (IPAC'18)*, Vancouver, BC, Canada, July 2018, paper WEPMF014.
- [7] B. Parker *et al.*, "BNL Direct Wind Superconducting Magnets," *IEEE Trans. Appl. Supercond.*, 2012, vol. 22 Issue 3, DOI: 10.1109/TASC.2011.2175693.
- [8] H. Witte, B. Parker, and R. Palmer, "Design of a Tapered Final Focusing Magnet for eRHIC," *IEEE Trans. Appl. Supercond.*, PP. 1-1. 10.1109/TASC.2019.2902982.